Photochromic Formazans: *X*-Ray Crystal Structure† Magnetic Resonance and Raman Spectra of 3-Methyl-1,5-diphenylformazan and 3-t-Butyl-1,5-diphenylformazan

Christopher W. Cunningham and Gary R. Burns*
Chemistry Department, Victoria University of Wellington, P.O. Box 600, Wellington, New Zealand
Vickie McKee
Department of Chemistry, University of Canterbury, Christchurch 1, New Zealand

The *X*-ray crystal structures of 3-methyl-1,5-diphenylformazan (**1**) and 3-t-butyl-1,5-diphenylformazan (**2**) have been determined. Magnetic resonance spectra, in both the solid state and in solution, and Raman spectra have been studied. $C_{14}H_{14}N_4$ (**1**) belongs to the monoclinic space group $P2_1/c$, a = 8.133(1), b = 19.085(4), c = 9.364(2) Å, β = 105.93°, U = 1 397.6(5) Å^3, Z = 4; the *anti*, s-*trans* configuration found for the solid state is also the thermodynamically preferred configuration in solution equilibrium. $C_{17}H_{20}N_4$ (**2**) belongs to the monoclinic space group $P2_1/c$, a = 11.235(3), b = 20.117(5), c = 14.176(3) Å, β = 92.14(2)°, U = 3 202(1) Å^3, Z = 8; the *syn*,s-*cis* configuration of the solid state is maintained in solution.

Formazans‡ have been known since the late nineteenth century when they were discovered and studied independently by Bamberger and his co-workers [1] and von Pechmann.[2] As a class of photochromic compound, formazans provide both organic and organometallic examples with the latter being the more widely investigated to date. Mercury(II) dithizonate§ remains one of the few commercially exploited photochromes while 1,3,5-triphenylformazan has recently found favour as a 'dramatic yet reliable' example of photo-isomerism for organic chemistry demonstrations.[3]

Formazans can in principle adopt four structures (Figure 1) ignoring isomers which are unlikely to occur due to serious steric crowding. This is as a result of *syn–anti* isomerisation about the C=N double bond and isomerisation about the C–N single bond designated s-*cis* and s-*trans* (Figure 1).

Otting and Neugebauer[4,5] have concluded that in solution the red and yellow formazans represent respectively *syn*,s-*cis* and *anti*,s-*trans* isomers. In the solid state, formazans crystallise as red or orange-yellow solids, with the *syn*,s-*cis*[6] or *syn*,s-*trans*[7,8] configurations¶ if red and the *anti*,s-*trans*[9–12] configuration if orange-yellow. We have recently determined[13] the structures of a pair of photochromes of a formazan equilibrium which we were able to isolate in the solid-state, as *anti*,s-*trans* and *syn*,s-*trans* respectively for the orange and red forms of 3-ethyl-1,5-diphenylformazan. In this work we report on 3-methyl-1,5-diphenylformazan, which crystallises as an orange formazan, and 3-t-butyl-1,5-diphenylformazan, which crystallises as a red formazan.

By 1955[14] over 500 formazans were known and this total has since increased to the present count of over a thousand. However, only eight have had their crystal structures determined,[6–13] and this present study is only the second in which the *syn*,s-*cis* configuration has been established. It is the first formazan with unsubstituted aromatic groups to have the *syn*,s-*cis* conformation unequivocally determined. Although the structure has been assumed to exist for half a century it is important, as we seek to explain why formazans adopt different structures on the basis of substitution at the three position, that there be no influence from substitution of the phenyl rings. The structure of (**2**) provides a useful analogue for 1,3,5-triphenylformazan which has been the subject of much study[15] although its crystal structure remains undetermined. The formazan (**2**) also provides an opportunity to investigate the quasi-aromatic ring postulated for 3-carboxymethylthio-1,5-diphenylformazan[16] whose solution structure is thought to be *syn*,s-*cis*.

The 3-methylformazan (**1**) is known to behave similarly to the closely related compound 3-ethyl-1,5-diphenylformazan. On irradiation in solution, the orange colour is promoted but it reverts to the red form on standing in the dark. All attempts to crystallise the dark-stable red isomer have been unsuccessful.

We present the crystal structure of (**1**) and (**2**) together with their magnetic resonance and Raman spectra.

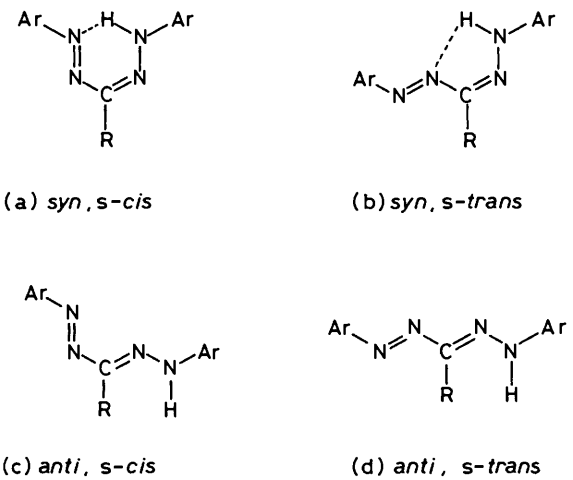

Figure 1. The principle isomers in the formazam system.

† *Supplementary data* (see Instructions for Authors, in the January issue). Full lists of bond lengths and angles, H-atom co-ordinates, and thermal parameters have been deposited at the Cambridge Crystallographic Data Centre.

‡ The generic name for compounds containing the –N=N–C=N–NH– backbone.

§ IUPAC: bis-(1,5-diphenylthiocarbazonato-*N*,*S*-)mercury(II).

¶ Following previous authors we use 'configuration' to describe the arrangement around a formal double bond and 'conformation' to describe the arrangement about a formal single bond.

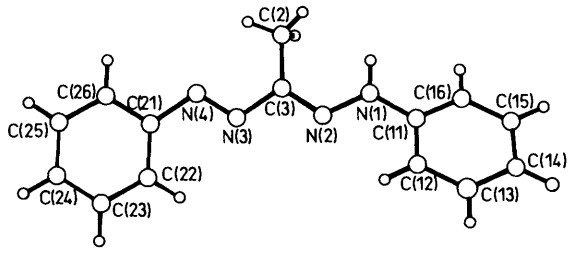

Figure 2. The molecular structure and nomenclature for 3-methyl-1,5-diphenylformazan (**1**).

Table 1. Fractional atomic co-ordinates ($\times 10^4$) for 3-methyl-1,5-diphenylformazan.

Atom	*x*	*y*	*z*
C(2)	−3 001(4)	1 783(2)	−287(4)
C(3)	−1 135(3)	1 830(1)	408(3)
N(1)	−1 348(3)	2 706(1)	1 979(2)
N(2)	−380(3)	2 253(1)	1 476(2)
N(3)	76(3)	1 419(1)	−19(2)
N(4)	−562(3)	984(1)	−1 039(2)
C(11)	−623(3)	3 118(1)	3 233(3)
C(12)	998(3)	2 996(1)	4 154(3)
C(13)	1 624(4)	3 417(2)	5 380(3)
C(14)	654(4)	3 946(2)	5 709(3)
C(15)	−962(4)	4 061(1)	4 805(3)
C(16)	−1 599(3)	3 657(1)	3 557(3)
C(21)	665(3)	573(1)	−1 494(3)
C(22)	2 422(4)	680(2)	−1 048(3)
C(23)	3 485(4)	255(2)	−1 575(3)
C(24)	2 810(4)	−280(2)	−2 549(3)
C(25)	1 082(4)	−392(2)	−3 004(3)
C(26)	14(4)	40(2)	−2 486(3)

Experimental

Syntheses.—3-methyl-1,5-diphenylformazan (**1**) was prepared following the method of Irving, Gill, and Cross.[17] The formazan was recrystallised from hot ethanol by the addition of water to yield orange needles in excellent yield (Found: C, 70.7; H, 5.8; N, 23.7. Calc. for $C_{14}H_{14}N_4$: C, 70.55; H, 5.92; N, 23.51%). 3-t-Butyl-1,5-diphenylformazan (**2**) was prepared following the method of Neugebauer and Trischmann.[18] The formazan was recrystallised from methanol–water (1:1) as dark red elongated needles with a striking metallic reflex (Found: C, 73.0; H, 7.5; N, 20.2. Calc. for $C_{17}H_{20}N_4$: C, 72.88; H, 7.19; N, 19.99%).

Crystal Structure Analysis and Data.—*3-Methyl-1,5-diphenylformazan* (**1**). An orange, regularly shaped crystal of dimensions 0.22 × 0.22 × 0.22 mm, monoclinic, a = 8.133(1), b = 19.085(4), c = 9.364(2) Å, β = 105.93°, U = 1 397.6(5) Å^3, space group $P2_1/c$, Z = 4, $F(000)$ = 503.9. 1.6° w-scans at 4.88° min^{-1} were used to collected 1 833 unique reflections in the range ($4 < 2\theta < 45°$) and, of these, 1 203 having $I < 3\sigma(I)$ were used for the structural analysis.

3-t-Butyl-1,5-diphenylformazan (**2**). A red crystal of irregular shape with dimensions 0.14 × 0.26 × 0.33 mm, monoclinic, a = 11.235(3), b = 20.117(5), c = 14.176(3) Å, β = 92.14(2)°, U = 3 202(1) Å^3; space group $P2_1/c$; Z = 8, $F(000)$ = 1 007.8. 1.6° w-scans at 4.88° min^{-1} were used to collect 4 176 unique reflections, 2 015 of these, which had $I < 3\sigma(I)$ were used in the subsequent calculations.

Intensity data for both crystals were collected at −100 °C with a Nicolet R3m four-circle diffractometer using graphite monochromated Mo-K_α radiation. Cell parameters were determined by least-squares refinement of 13 accurately centred reflections ($2\theta > 15°$). Crystal stability was monitored by recording 3 check reflections every 100 reflections and no significant variations were observed. The data sets were corrected for Lorentz-polarisation effects but no absorption corrections were applied.

Both structures were solved by direct methods, using the program SOLV, and refined by blocked-cascade least squares methods. The refinement of (**1**) converged with R = 0.045 and R' = 0.066 while (**2**) converged with R = 0.061 and R' = 0.091. All non-hydrogen atoms were refined anisotropically and hydrogen atoms [except H(1) in (**1**) and H(11) and H(21) in (**2**)] were inserted at calculated positions using a riding model with thermal parameters equal to 1.2U of their carrier atoms. H(1), H(11), and H(21) were located from difference Fourier maps, inserted at this positions and not further refined. The function minimised in the refinement was $\Sigma w(|F_o| - |F_c|)^2$ where $w = [\sigma^2(F_o) + gF_o^2]^{-1}$ and g = 0.0026. Final difference maps showed no features greater than ~0.3 electron Å^{-3}.

All programs used for data collection and structure solution are contained in the SHELXTL (Version 4) package.*

General Methods.—Solid state ^{13}C n.m.r. spectra were recorded at 50.3 MHz with a Varian Associates XL-200 spectrometer using a standard CP/MAS probe. Powdered samples (*ca.* 300 mg) were packed in Kel-F rotors and spun using MAS frequencies between 2 and 3 kHz for (**1**) and at 10 kHz for (**2**). The combined techniques of high power proton decoupling and single contact cross polarisation (CP) were employed. Typical contact times of 50 ms were used, with recycle delays of 1.2 s. The number of transients acquired was of the order of 1 000.

Solution spectra were recorded at 20.00 MHz with a Varian Associates FT-80A spectrometer employing proton decoupling. In all cases either deuterated solvents or D_2O capillary tubes provided the spin lock. Typical spectral parameters employed were: spectral width 5 000 Hz, acquisition time 1.023 s, pulse width 4 μs. Samples of *ca.* 200 mg were used in 5 mm o.d. tubes with tetramethylsilane as the internal standard. Care was taken to protect the spectroscopic solutions from the effect of light.

Raman spectra were recorded using a Spex 1401 spectrometer equipped with a Thorn EMI 6256 photomultiplier tube used in the photon counting mode. A Spectra-Physics 164-01 Krypton Ion laser was used as the Raman scattering source, operating at a wavelength of 647 nm. Band wavenumbers were calibrated using the emission spectrum of neon and typical slit widths of 200 μm were employed, giving a bandpass of 2 cm^{-1} at 647 nm. Samples were studied as crystals or in capillary tubes. Pressed discs diluted in potassium bromide were also used effectively to eliminate fluorescence. Spectra were recorded at room temperature using laser powers of less than 50 mW at the sample to avoid photo-decomposition.

Electronic absorption spectra were recorded with a Shimadzu Model 160 u.v.–visible spectrophotometer. Solvents were of spectroscopic grade or purified by standard methods.

Microanalyses were performed by Professor A. D. Campbell of the University of Otago.

Results and Discussion

Crystal Structures.—The molecular structure and atomic nomenclature for (**1**) and (**2**) are given in Figures 2 and 3. The final fractional atomic coordinates are given in Tables 1 and 2). The bond lengths and bond angles are given in Tables 3 and 4.

The calculated bond lengths reveal a marked delocalisation

* G. M. Sheldrick, SHELXTL User Manual, Revision 4, Nicolet XRD Corporation, Madison, Wisconsin, 1984.

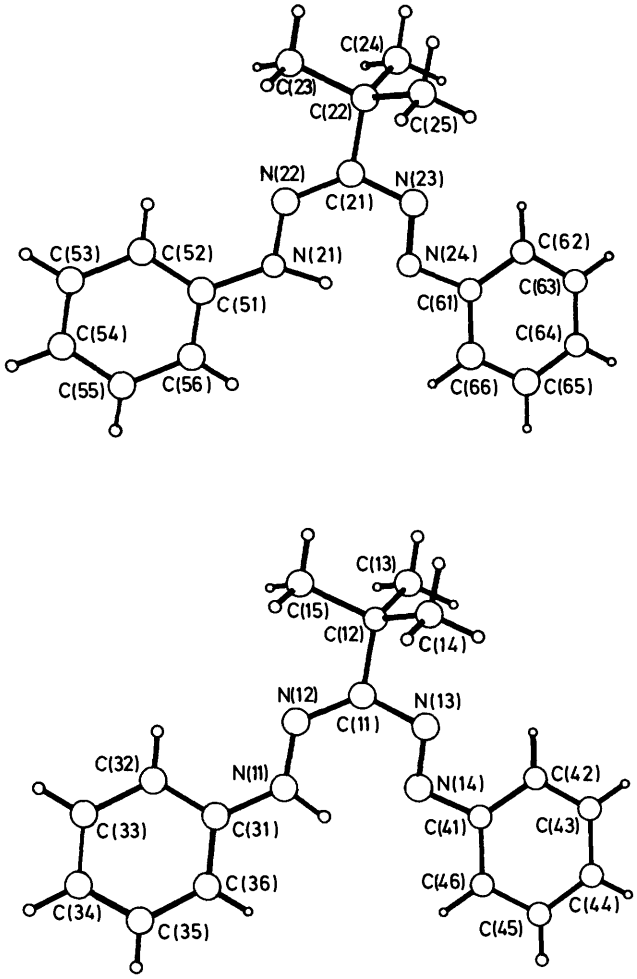

Figure 3. The molecular structure and nomenclature for 3-t-butyl-1,5-diphenylformazan (**2**).

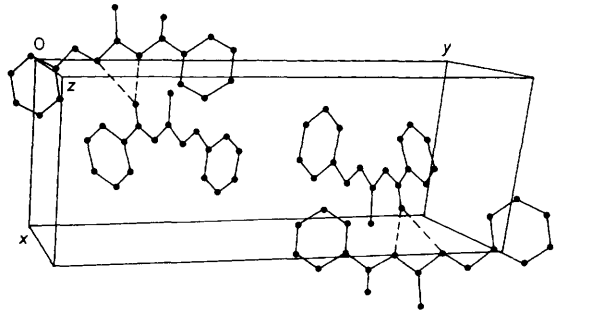

Figure 4. A unit-cell projection for 3-methyl-1,5-diphenylformazan.

of electrons over the N–N–C–N–N formazan backbone for (**1**) and (**2**). While the formal double bonds are clearly extended in comparison with isolated double bonds, the formal single bonds are noticeably shortened. For comparison, bond lengths and bond angles for the formazans of similar configuration are given, as are those for the *syn*,s-*trans* red isomer of 3-ethyl-1,5-diphenylformazan (see Table 5). Bond orders have been calculated after the method of Burke-Laing and Laing.[19] For (**1**) C=N, bond order = 1.8; C–N, 1.2; N=N, 1.8; N–N, 1.4; for (**2**) C=N, 1.8; C–N, 1.2; N=N, 1.8; N–N, 1.4. It can be seen that while there is extensive delocalisation of the π-electrons for all of the formazans compared, the double-bond and single-bond character of the skeleton is clearly maintained as the 3-

Table 2. Fractional atomic co-ordinates ($\times 10^4$) for 3-t-butyl-1,5-diphenylformazan.

Atom	*x*	*y*	*z*
N(14)	1 157(5)	4 214(2)	4 914(4)
N(13)	339(5)	4 137(2)	4 265(4)
C(11)	352(5)	4 658(3)	3 553(4)
C(12)	−590(6)	4 538(3)	2 766(4)
C(13)	−1 812(6)	4 476(3)	3 184(4)
C(14)	−292(6)	3 899(3)	2 257(4)
C(15)	−604(6)	5 115(3)	2 061(4)
N(12)	1 084(4)	5 162(2)	3 459(3)
N(11)	1 960(4)	5 258(2)	4 111(3)
C(41)	1 111(6)	3 712(3)	5 618(4)
C(42)	111(6)	3 331(3)	5 763(4)
C(43)	143(6)	2 853(3)	6 471(4)
C(44)	1 169(7)	2 764(3)	7 026(4)
C(45)	2 161(7)	3 146(3)	6 888(4)
C(46)	2 127(6)	3 630(3)	6 187(4)
C(31)	2 765(5)	5 769(3)	3 985(4)
C(32)	2 675(6)	6 217(3)	3 240(4)
C(33)	3 542(6)	6 704(3)	3 147(5)
C(34)	4 501(6)	6 741(3)	3 778(4)
C(35)	4 592(6)	6 298(3)	4 518(4)
C(36)	3 741(6)	5 818(3)	4 621(4)
N(24)	3 610(4)	10 415(2)	4 120(3)
N(23)	4 497(4)	10 205(3)	3 661(3)
C(21)	4 655(6)	9 513(3)	3 629(4)
C(22)	5 666(6)	9 311(3)	2 996(4)
C(23)	5 873(6)	8 562(3)	3 054(5)
C(24)	6 816(6)	9 684(3)	3 279(5)
C(25)	5 297(6)	9 495(4)	1 974(4)
N(22)	4 039(5)	9 050(2)	4 033(3)
N(21)	3 124(4)	9 204(2)	4 565(3)
C(61)	3 507(6)	11 124(3)	4 147(4)
C(62)	4 411(6)	11 558(3)	3 908(4)
C(63)	4 208(7)	12 235(3)	3 993(5)
C(64)	3 148(7)	12 479(3)	4 302(5)
C(65)	2 266(6)	12 044(3)	4 540(4)
C(66)	2 437(6)	11 364(3)	4 474(4)
C(51)	2 530(6)	8 693(3)	5 024(4)
C(52)	2 899(6)	8 036(3)	4 971(4)
C(53)	2 282(6)	7 555(3)	5 444(5)
C(54)	1 338(7)	7 726(3)	5 978(5)
C(55)	950(6)	8 377(4)	6 022(4)
C(56)	1 554(6)	8 859(3)	5 548(4)

substituent, and therefore the configuration, changes from methyl to ethyl and finally to t-butyl. While substitution and configuration do not have a profound effect on the bond orders, the subtle differences which are seen are reflected in the vibrational spectra of the systems.

The structure of (**1**) closely resembles other orange formazans which assume the *anti*,s-*trans* configuration.[13] The N–N–C–N–N backbone is planar and the phenyl rings are inclined to this plane [the angle between C(11)–C(16) and the mean plane C(21)–C(26) = 27°]. Delocalisation of electrons extends to the phenyl rings with N–C(phenyl) bond lengths of 1.402 and 1.423 Å which represent bond orders of *ca.* 1.2.

Selected intermolecular distances for (**1**) are listed in Table 6 and a view of the unit cell is given in Figure 4. There is a significantly short intermolecular hydrogen bond of 2.31 Å between H(1) and N(2). This distance is less than the sum of the van der Waals radii of Bondi[20] (2.95 Å). The C(2)–C(3) distance of 1.48 Å is clearly a single bond and therefore delocalisation does not extend into the methyl substituent.

The structure of (**2**) differs significantly from the only other *syn*,s-*cis* configuration structurally confirmed for a formazan. Dijkstra *et al.*[6] report a mesomeric structure for 1,5-bis(2,6-dimethylphenyl)-3-nitroformazan. However, the structure of (**2**)

Table 3. Bond lengths/Å and bond angles/° for 3-methyl-1,5-diphenylformazan.

(*a*) Bond lengths

C(2)–C(3)	1.480(4)	C(3)–N(2)	1.302(3)
C(3)–N(3)	1.400(4)	N(1)–N(2)	1.339(3)
N(1)–C(11)	1.402(3)	N(3)–N(4)	1.264(3)
N(4)–C(21)	1.423(4)	C(11)–C(12)	1.383(4)
C(11)–C(16)	1.382(4)	C(12)–C(13)	1.379(4)
C(13)–C(14)	1.368(5)	C(14)–C(15)	1.372(4)
C(15)–C(16)	1.377(4)	C(21)–C(22)	1.390(4)
C(21)–C(26)	1.381(4)	C(22)–C(23)	1.372(5)
C(23)–C(24)	1.378(5)	C(24)–C(25)	1.368(5)
C(25)–C(26)	1.379(5)		

(*b*) Bond angles

C(2)–C(3)–N(2)	125.8(3)	C(2)–C(3)–N(3)	123.9(2)
N(2)–C(3)–N(3)	110.2(2)	N(2)–N(1)–C(11)	120.3(2)
C(3)–N(2)–N(1)	118.2(2)	C(3)–N(3)–N(4)	114.1(2)
N(3)–N(4)–C(21)	114.3(2)	N(1)–C(11)–C(12)	122.6(2)
N(1)–C(11)–C(16)	117.8(2)	C(12)–C(11)–C(16)	119.7(2)
C(11)–C(12)–C(13)	119.5(3)	C(12)–C(13)–C(14)	120.9(2)
C(13)–C(14)–C(15)	119.6(3)	C(14)–C(15)–C(16)	120.5(3)
C(11)–C(16)–C(15)	119.9(2)	N(4)–C(21)–C(22)	125.3(2)
N(4)–C(21)–C(26)	115.9(2)	C(22)–C(21)–C(26)	118.9(3)
C(21)–C(22)–C(23)	120.2(3)	C(22)–C(23)–C(24)	120.0(3)
C(23)–C(24)–C(25)	120.7(3)	C(24)–C(25)–C(26)	119.3(3)
C(21)–C(26)–C(25)	121.0(3)		

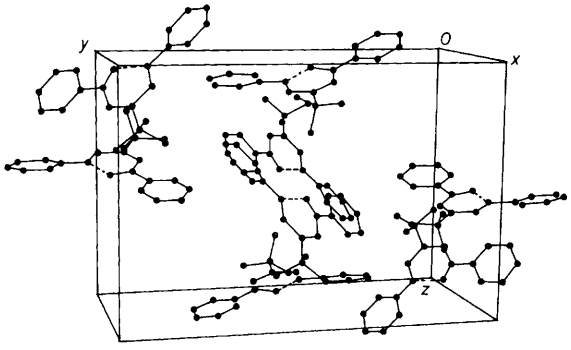

Figure 5. A unit-cell projection for 3-t-butyl-1,5-diphenylformazan.

can not be described as mesomeric. The two N–N bond lengths are dissimilar as are the two C–N bond lengths. The imino proton is not symmetrically located equidistant from N(1) and N(5) and it does not share the plane of the N–N–C–N–N backbone. The phenyl rings are inclined to the plane of the backbone. The angle between C(41)–C(46) and the mean plane of C(31)–C(36) = 12.1°; the angle between C(61)–C(66) and the mean plane of C(51)–C(56) = 19.1°. This inclination does not preclude delocalisation of electrons into the phenyl rings and the N–C(phenyl) bond distances of less than 1.43 Å confirm some delocalisation. A corresponding delocalisation into the ring is not seen for the nitro-formazan structure; substitution of the phenyl rings was held to account for the twisting of the phenyl rings out of the plane. The C(11)–C(12) distance of 1.52 Å, however, is clearly a single bond indicating that delocalisation of electrons into the backbone and phenyl rings does not extend to the t-butyl substituent.

The *X*-ray analysis shows that there are two unique molecules of (**2**) in each unit cell. There are also significant intramolecular hydrogen bonds in the molecules of (**2**). Selected intramolecular bond distances for (**2**) are listed in Table 7 and a view of the unit cell is given in Figure 5. The H(11)–N(14) distance of 1.85 Å and the H(21)–N(24) distance of 1.58 Å are considerably less than the sum of the van der Waals radii of Bondi[20] (2.95 Å). The formazan is therefore effectively locked into the *syn*,s-*cis* configuration.

^{13}C *N.m.r. Spectra.*—The ^{13}C n.m.r. resonances in the solid state and in solution for (**1**) and (**2**) are listed in Tables 8 and 9. Assignments in the solid-state are based on the use of short contact times to identify quaternary carbon signals, and TOSS experiments and multiple spinner speeds to remove sidebands. Assignments in solution are based on gated spin echo and selective decoupling experiments.

In solid-state n.m.r. spectroscopy some of the motional degrees of freedom are quenched allowing the identification of different conformers. The solid-state ^{13}C n.m.r. spectra confirm that, while (**1**) and (**2**) each exist in pure configurations, they do not exist in the same configuration. For (**1**) discrete signals for C(11) and C(21) are observed confirming their non-equivalence and only one signal for the methyl substituent is observed for the *anti*,s-*trans* configuration as established by the *X*-ray analysis. For (**2**) only one signal is observed for the quaternary aromatic carbon atoms due to their equivalence in the *syn*,s-*cis* configuration; one set of signals only is seen for the t-butyl group. The shift in the C(3) signals for (**1**) and (**2**) reflects the difference in C=N bond order with the greater electron density of (**1**) giving the downfield resonance when compared with (**2**).

In solution both the *anti*,s-*trans* and *syn*,s-*cis* configurations yield equivalent aromatic carbon resonances as tautomerism is fast on the n.m.r. timescale. The *syn*,s-*trans* configuration, however, yields discrete signals for the aromatic carbon atoms as they are not equivalent and are unaffected by tautomerism. The resonances for the 3-substituents also provide a useful method for analysing the conformational integrity of the sample. For (**1**) two configurations are apparent giving the two 3-methyl resonances between 6 and 16 ppm. The *anti*,s-*trans* form is in equilibrium with the *syn*,s-*trans* form as evidenced by the more complicated pattern of phenyl resonances in all of the solvents studied with the exception of the methanol spectrum which emulates the solid-state spectrum: ($CDCl_3$) 129.3, 126.3, 118.4 for *anti*,s-*trans*; 130.5, 129.0, 122.9, 122.1, 114.4 for *syn*,s-*trans* (the *p*-phenyl carbon atoms are equivalent in both forms). Isomer ratios can be gauged and are listed in Table 8. Further evidence for the existence of an equilibrium comes from the electronic absorption spectra shown in Figure 6. These spectra clearly demonstrate that both an orange and a red form are present in differing concentrations in all solvents except methanol. For (**2**) the *syn*,s-*cis* configuration occurs in solution in both protic and aprotic solvents and the resonances in solution closely resemble those of the solid state. The electronic absorption spectra for (**2**) are shown in Figure 7. There is no change in absorption maximum for the solvents studied confirming that there is no appreciable contribution from an orange conformer for (**2**).

Raman Spectra.—The band centre wavenumbers for the normal modes of vibration of (**1**) and (**2**) are listed in Table 10 and typical Raman spectra are shown in Figures 8 and 9. Comparison of the two spectra is useful as they exemplify orange *anti*,s-*trans* and red *syn*,s-*cis* formazans. The Raman spectrum has previously been reported[21] for 3-methyl-1,5-diphenylformazan at a different exciting wavelength and is included for comparison. No Raman spectra have been reported for (**2**).

The Raman spectrum of (**1**) closely resembles that already reported for the orange isomer of 3-ethyl-1,5-diphenylformazan. The two most intense bands at 1 413 and 1 145 cm^{-1} in (**1**) can be assiged to $\nu_{N=N}$ and ν_{N-N} respectively [1 411 and 1 147 cm^{-1} in (**3**)]. The bands at 1 321, 1 315, and 1 306 cm^{-1} are a

Table 4. Bond lengths/Å and bond angles/° for 3-t-butyl-1,5-diphenylformazan.

(*a*) Bond lengths

N(14)–N(13)	1.279(7)	N(14)–C(41)	1.422(7)
N(13)–C(11)	1.404(7)	C(11)–N(12)	1.316(7)
N(12)–N(11)	1.340(7)	N(11)–C(31)	1.386(8)
C(41)–C(42)	1.382(9)	C(41)–C(46)	1.383(8)
C(42)–C(43)	1.390(9)	C(43)–C(44)	1.383(10)
C(44)–C(45)	1.374(10)	C(45)–C(46)	1.391(9)
C(31)–C(32)	1.389(8)	C(31)–C(36)	1.397(9)
C(32)–C(33)	1.391(9)	C(33)–C(34)	1.376(9)
C(34)–C(35)	1.377(9)	C(35)–C(36)	1.371(9)
N(24)–N(23)	1.282(7)	N(24)–C(61)	1.431(8)
N(23)–C(21)	1.405(8)	C(21)–N(22)	1.305(8)
N(22)–N(21)	1.334(7)	N(21)–C(51)	1.401(8)
C(61)–C(62)	1.390(9)	C(61)–C(66)	1.390(9)
C(62)–C(63)	1.388(9)	C(63)–C(64)	1.375(10)
C(64)–C(65)	1.373(10)	C(65)–C(66)	1.386(9)
C(51)–C(52)	1.388(8)	C(51)–C(56)	1.387(9)
C(52)–C(53)	1.379(9)	C(53)–C(54)	1.370(10)
C(54)–C(55)	1.381(10)	C(55)–C(56)	1.374(9)

(*b*) Bond angles

N(13)–N(14)–C(41)	114.5(5)	N(14)–N(13)–C(11)	116.5(5)
N(13)–C(11)–N(12)	129.2(5)	C(11)–N(12)–N(11)	119.2(6)
N(12)–N(11)–C(31)	119.0(5)	N(14)–C(41)–C(42)	123.3(5)
N(14)–C(41)–C(46)	116.3(5)	C(42)–C(41)–C(46)	120.3(5)
C(41)–C(42)–C(43)	119.5(6)	C(42)–C(43)–C(44)	119.9(6)
C(43)–C(44)–C(45)	120.7(6)	C(44)–C(45)–C(46)	119.5(6)
C(41)–C(46)–C(45)	120.0(6)	N(11)–C(31)–C(32)	123.4(5)
N(11)–C(31)–C(36)	118.0(5)	C(32)–C(31)–C(36)	118.6(6)
C(31)–C(32)–C(33)	119.8(6)	C(32)–C(33)–C(34)	120.7(6)
C(33)–C(34)–C(35)	119.6(6)	C(34)–C(35)–C(36)	120.3(6)
C(31)–C(36)–C(35)	121.0(6)	N(23)–N(24)–C(61)	114.1(5)
N(24)–N(23)–C(21)	116.4(5)	N(23)–C(21)–N(22)	128.6(6)
C(21)–N(22)–N(21)	121.0(5)	N(22)–N(21)–C(51)	118.9(5)
N(24)–C(61)–C(62)	123.9(6)	N(24)–C(61)–C(66)	115.3(5)
C(62)–C(61)–C(66)	120.8(6)	C(61)–C(62)–C(63)	118.1(6)
C(62)–C(63)–C(64)	121.7(7)	C(63)–C(64)–C(65)	119.5(6)
C(64)–C(65)–C(66)	120.6(6)	C(61)–C(66)–C(65)	119.3(6)
N(21)–C(51)–C(52)	121.7(6)	N(21)–C(51)–C(56)	118.2(5)
C(52)–C(51)–C(56)	120.1(6)	C(51)–C(52)–C(53)	119.0(6)
C(52)–C(53)–C(54)	120.4(6)	C(53)–C(54)–C(55)	121.1(7)
C(54)–3C(55)–C(56)	118.9(6)	C(51)–C(56)–C(55)	120.5(6)

reflection of the C–N bond order in (**1**). The corresponding bands appear at 1 331, 1 321, and 1 306 cm^{-1} in (**3**) which has a longer C=N bond and a shorter C–N bond length but which has an average C–N bond order equal to that of (**1**).

Weaker scattering is observed for (**2**) due to the increased self absorption of the sample. The lower stability of (**2**) also requires the use of decreased laser powers. It is still evident that the Raman spectrum of (**2**) differs significantly from that of (**1**). The most intense band at 1 363 cm^{-1} has shifted from 1 413 cm^{-1} in (**1**) as the N=N bond length increases from 1.264 Å in (**1**) to 1.279 and 1.282 Å in (**2**). The band at 1 159 cm^{-1} is assigned to the ν_{N-N} normal mode but does not have the intensity of the corresponding band in (**1**). The band at 1 601 cm^{-1} is assigned to vibrations of the phenyl ring and is relatively more intense than the corresponding bands in (**1**) which are weaker and are centred at 1 598, 1 590, and 1 580 cm^{-1}.

Conclusions

3-Methyl-1,5-diphenylformazan exists in the *anti*,s-*trans* configuration in the solid-state. In methanol solution this form is maintained; in aprotic solvents, however, this form is in equilibrium with the *syn*,s-*trans* configuration. This behaviour

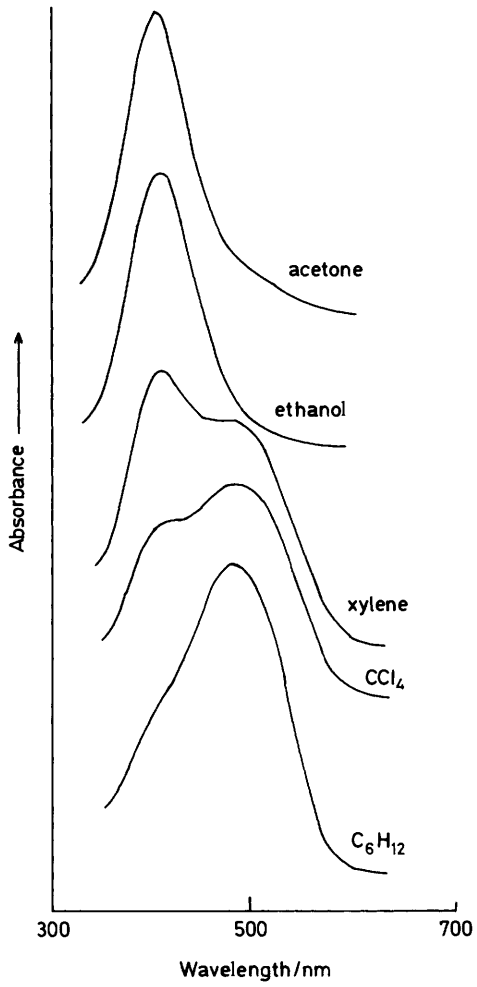

Figure 6. U.v.–visible absorption spectra of 3-methyl-1,5-diphenylformazan.

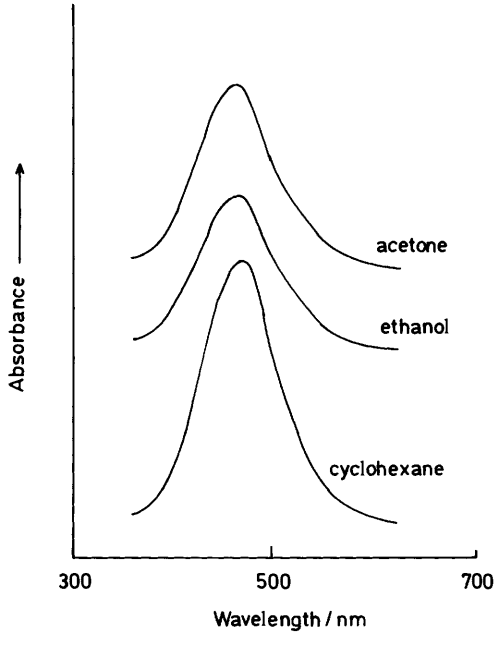

Figure 7. U.v.–visible absorption spectra of 3-t-butyl-1,5-diphenylformazan.

Table 5. A comparison of some bond angles and bond lengths for selected 3-substituted-1,5-diphenylformazan –N=N–C=N–N– backbones.

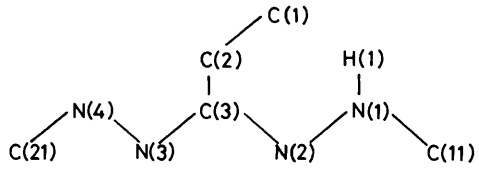

	3-Methyl-[a]	3-Ethyl-[a]		3-t-Butyl-[a]		3-Nitro-[b]
		Orange	Red	A	B	
Bond lengths/Å						
C(1)–C)2)		1.525(3)	1.515(16)			
C(2)–C(3)	1.480(4)	1.496(2)	1.520(17)			
C(3)–N(2)	1.302(3)	1.298(2)	1.308(15)	1.316(7)	1.305(8)	1.322(5)
C(3)–N(3)	1.400(4)	1.403(2)	1.379(15)	1.404(7)	1.405(8)	1.346(5)
N(1)–N(2)	1.339(3)	1.337(2)	1.361(13)	1.340(7)	1.334(7)	1.301(5)
N(1)–C(11)	1.402(3)	1.400(2)	1.389(15)	1.386(8)	1.401(8)	1.436(5)
N(3)–N(4)	1.264(3)	1.269(2)	1.265(13)	1.279(7)	1.282(7)	1.298(5)
N(4)–C(21)	1.423(4)	1.422(3)	1.417(15)	1.422(7)	1.431(8)	1.421(5)
Bond angles/°						
C(1)–C(2)–C(3)	111.0(2)	114.4(10)				
C(2)–C(3)–N(2)	125.8(3)	126.8(2)	116.8(10)			
C(2)–C(3)–N(3)	123.9(2)	122.4(2)	124.5(10)			
N(2)–C(3)–N(3)	110.2(2)	110.7(1)	118.6(10)	129.2(5)	128.6(6)	136.5(5)
N(2)–N(1)–C(11)	120.3(2)	120.2(1)	120.0(9)	119.0(5)	118.9(5)	116.0(5)
C(3)–N(2)–N(1)	118.2(2)	118.0(1)	117.5(9)	119.2(5)	121.0(5)	117.0(5)
C(3)–N(3)–N(4)	114.1(2)	113.5(1)	112.6(9)	116.5(5)	116.4(5)	117.2(5)
N(3)–N(4)–C(21)	114.3(2)	114.5(1)	113.3(9)	114.5(5)	114.1(5)	116.7(5)
N(4)–C(21)–C(22)	125.3(2)	124.9(2)	125.9(10)	123.3(5)	123.9(6)	121.7(5)
N(4)–C(21)–C(26)	115.9(2)	115.1(2)	115.6(10)	116.3(5)	115.3(5)	115.7(5)
N(1)–C(11)–C(12)	122.6(2)	121.9(2)	116.7(10)	123.4(5)	121.7(6)	122.9(5)
N(1)–C(11)–C(16)	117.8(2)	118.1(2)	124.1(10)	118.0(5)	118.2(5)	115.6(5)

[a] This paper. [b] Ref. 6.

Table 6. Selected inter- and intra-molecular distances Å and bond angles ° for 3-methyl-1,5-diphenylformazan.

N(1′)–H(1′)	0.960				
N(1′)–N(2′)	1.339	119.8			
N(1′)–C(11′)	1.402	119.9	120.3		
N(1′)–N(2)	3.183	20.3	130.2	106.8	
N(1′)–N(3)	3.429	25.5	128.0	106.4	39.0
		H(1′)	N(2′)	C(11′)	N(2)
H(1′)–N(1′)	0.960				
H(1′)–N(2)	2.307	151.4			
H(1′)–N(3)	2.596	145.3	53.4		
		N(1′)	N(2)		

Table 7. Selected inter- and intra-molecular distances (Å) for 3-t-butyl-1,5-diphenylformazan.

H(11)–N(14)	1.85
N(11)–N(14)	2.57
H(21)–N(24)	1.58
N(21)–N(24)	2.58

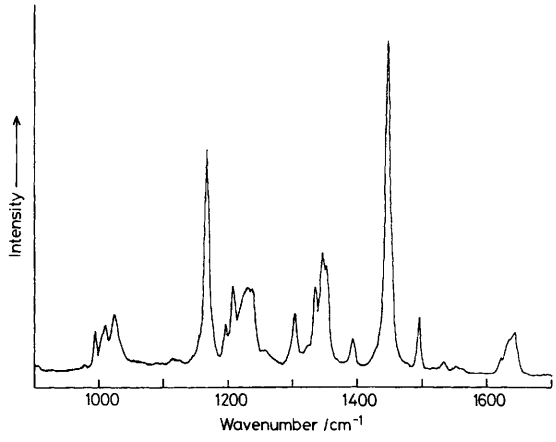

Figure 8. Raman spectrum of crystalline 3-methyl-1,5-diphenylformazan.

closely parallels that of 3-ethyl-1,5-diphenylformazan and would seem to be characteristic of orange 3-substituted 1,5-diphenylformazans in general.

The methyl substituent is clearly the feature which determines the conformation of (**1**) allowing the open configuration in the solid which is further stabilised by an intermolecular hydrogen bond. In solution the formation of an equilibrium involving the closed structure is evidenced by the absorption and magnetic resonance spectra. The red form of (**1**) is clearly *syn*,s-trans and not *syn*,s-*cis* which is seen when the 3-substituent is bulky. While the red form of (**1**) becomes increasingly important in $CDCl_3$ and C_6D_6 solutions the orange form is still apparent in appreciable concentration, even in aprotic solvents in the dark. It has been shown[22,23] that red forms are promoted by traces of acid but destabilised by exposure to light.

3-t-Butyl-1,5-diphenylformazan exists in the *syn*,s-*cis* configuration in the solid state. This form is maintained in solution as the t-butyl substituent does not favour the formation of a *trans* arrangement around the C=N double bond.

Table 8. ^{13}C N.m.r. spectra of 3-methyl-1,5-diphenylformazan (δ in ppm from TMS)

State	$-CH_3$	Intensity (%)	C(3)	C(11)	C(21)	Aromatic
Solid	7.8	100	155.8	153.1	144.0	114.7
						124.1
						130.2
MeOH	7.9	100	154.7		149.8	130.1
						127.0
						119.5
$(CD_3)_2CO$	7.4	80	155.0		149.5	129.9
						126.9
						114.7
	15.5	18			147.5	*a*
$CDCl_3$	6.6	58	154.2		149.5	129.3
						126.3
						118.3
	16.1	42	152.1	147.1	143.2	130.5
						129.0
						122.9
						122.1
						114.4
C_6D_6	6.1	33	154.1		148.7	129.4
						126.5
						118.8
	16.2	67	153 wk	147.1	144 wk	130.5
						127.5
						123.3
						122.2
						114.6

[a] Weak bands.

Table 9. ^{13}C N.m.r. spectra for 2-t-butyl-1,5-diphenylformazan (δ in ppm from TMS).

State	Bu^t	C(3)	C(11)	C(21)	Aromatic
Solid	38	31	149.8	146.5	129.4
					123.8
					120.3
					114.6
$CDCl_3$	38.05	29.88	150.21	148.21	118.35
					129.30
					126.73
$(CD_3)_2CO$	38.56	30.01	150.86	149.41	119.24
					130.18
					127.70

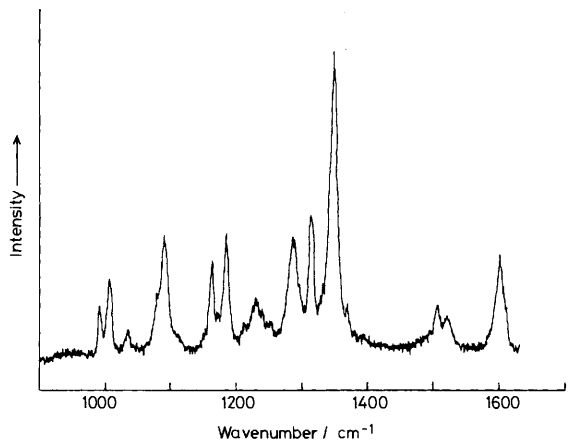

Figure 9. Raman spectrum of crystalline 3-t-butyl-1,5-diphenylformazan.

Table 10. Band centre wavenumbers (cm^{-1}) for the Raman-active phonons of (**1**) and (**2**)

3-Methyl		3-t-Butyl
solid 647.1	solid 422	solid 647.1
1 598	1 605	1 601
1 590		
1 580		
1 511		1 522
1 494	1 500	1 505
1 456	1 464	
1 413	1 412	1 344
1 359	1 370	1 363
1 321	1 320	1 310
1 315		
1 306		
1 273	1 282	1 279
1 206	1 208	1 222
1 185	1 196	1 176
1 172		1 169
1 145	1 148	1 159
	1 018	1 085
1 011	1 010	1 030
996		1 001
981		984

The t-butyl substituent is clearly the feature which determines the conformation of the formazan due to its steric effect at the 3-position. The effect of intra- or inter-molecular hydrogen bonding would appear to play a secondary role. The stabilising influence of an all-planar ring system would also appear to play a role.

The combined techniques of n.m.r. and Raman spectroscopy make it possible to monitor changes in the formazan structure due to simple 3-substitution. Differences in the C=N bond orders are reflected in the solid-state ^{13}C n.m.r. spectra shifts of the C(3) signals. The Raman active phonons of formazans are sensitive to conformational differences in the system. The band centre wavenumber for the normal modes based mainly on the N=N function shows a marked shift depending upon the configuration of the formazan. Solution n.m.r. spectroscopy allows the straightforward characterisation of the equilibrium configurations of the formazan in different solvents; in particular the red *syn,s-trans* form has a characteristic pattern of signals compared with the more symmetric forms.

Acknowledgements

One of the authors, C. W. C. is grateful to the Maori Education Foundation for the granting of a Queen Elizabeth II Post Graduate Scholarship during the research for this paper. We are also grateful to Dr. R. H. Newman and Dr. K. Morgan of the DSIR for recording solid-state magnetic resonance spectra.

References

1 E. Bamberger and E. W. Wheelwright, *Chem. Ber.*, 1892, **25**, 3201.
2 H. von Pechmann, *Chem. Ber.*, 1892, **25**, 3175.
3 E. F. Silversmith, *J. Chem. Educ.*, 1988, **65(1)**, 70.
4 W. Otting and F. A. Neugebauer, *Chem. Ber.*, 1969, **102**, 2520.
5 W. Otting and F. A. Neugebauer, *Z. Naturforsch., Teil B*, 1968, **23**, 1064.
6 E. Dijkstra, A. T. Hutton, H. M. N. H. Irving, and L. R. Nassimbeni, *Acta Crystallogr., Sect. B*, 1982, **38**, 535.
7 J. Preuss and A. Gieren, *Acta Crystallogr., Sect. B*, 1975, **31**, 1276.
8 A. T. Hutton, H. M. N. H. Irving, L. R. Nassimbeni, and G. Gafner, *Acta Crystallogr., Sect. B*, 1979, **35**, 1354.
9 Yu. Omel'chenko, Yu. D. Kondrashev, S. L. Ginsburg, and M. G. Neiganz, *Cristallografiya*, 1974, **19**, 522.

10 M. Laing, *J. Chem. Soc., Perkin Trans. 2*, 1977, 1248.
11 J. Guillerez, C. Pascard, and T. Prange, *J. Chem. Res.*, 1978, (*S*), 308; (*M*), 1978, 3934.
12 A. T. Hutton, H. M. N. H. Irving, and L. R. Nassimbeni, *Acta Crystallogr., Sect. B*, 1980, **36**, 2071.
13 G. R. Burns, C. W. Cunningham, and V. McKee *J. Chem. Soc., Perkin Trans. 2*, 1988, 1275.
14 A. W. Nineham, *Chem. Rev.*, 1955, **55**, 355.
15 R. Kuhn and H. M. Weitz, *Chem. Ber.*, 1953, **86**, 1199; H. Langbein, *J. Prakt. Chem.*, 1979, **321**, 665; P. V. Fischer, B. L. Kaul, and H. Zollinger, *Helv. Chim. Acta*, 1968, **51**, 1449; U. W. Grummt and H. Langbein, *J. Photochem.*, 1981, **15**, 329; J. W. Lewis and C. Sandorfy, *Can. J. Chem.*, 1983, **61**, 809; M. F. Kovalenko, P. B. Kurapov, and I. I. Grandberg, *Zh. Org. Khim.*, 1987, **23(5)**, 1070.
16 A. T. Hutton, H. M. N. H. Irving, K. R. Koch, L. R. Nassimbeni, *J. Chem. Soc., Chem. Commun.*, 1979, 57.
17 H. M. N. H. Irving, J. B. Gill, and W. R. Cross, *J. Chem. Soc.*, 1960, 2087.
18 F. A. Neugebauer and H. Trischmann, *Liebigs Ann. Chem.*, 1967, **706**, 107.
19 M. Burke-Laing and M. Laing, *Acta Crystallogr., Sect. B*, 1976, **B32**, 3216.
20 A. Bondi, *J. Phys. Chem.*, 1964, **68(3)**, 411.
21 I. I. Kukushkina, E. N. Yurchenko, D. K. Arkhipenko, and B. A. Orekhov, *J. Phys. Chem.*, 1972, **46(7)**, 963.
22 A. T. Hutton and H. M.N. H. Irving, *J. Chem. Soc., Perkin Trans. 2*, 1982, 1117.
23 Y. Sueshi and N. Nishimura, *Bull. Chem. Soc. Jpn.*, 1983, **56**, 2598.

Received 24*th August* 1988; *Paper* 8/03429J